

after reaction 4. (Reaction 4 was assumed to be complete when the  $\text{Cl}^+$  signal was no longer detected.) Although initially the HCl was evenly distributed throughout the ice, the ice remaining after reaction contained less than 5% of the original HCl. This suggests that almost all of the HCl in the ice was available for reaction with  $\text{N}_2\text{O}_5$ .

The mechanism for the reactions of  $\text{N}_2\text{O}_5$  on ice and HCl-ice surfaces is not known. The rapidity of heterogeneous reactions such as reactions 1 through 4 has led to the suggestion that these reactions are catalyzed by  $\text{H}^+$  in the ice (3, 5). The facile reaction of  $\text{N}_2\text{O}_5$  with HCl at low temperatures even in the absence of ice may have mechanistic implications. We cannot rule out possible water impurities below our detection limit (0.01 mtorr) that could influence the reaction mechanism.

Our results indicate that heterogeneous reactions of  $\text{N}_2\text{O}_5$  with HCl and  $\text{H}_2\text{O}$  occur readily at 185 K, providing a sink for  $\text{NO}_x$  in the form of condensed-phase  $\text{HNO}_3$  and producing photochemically active gas-phase  $\text{ClNO}_2$ . To the extent that the surfaces studied here are similar to PSCs, reactions 3 and 4 may contribute to the photochemical mechanism responsible for ozone depletion in the Antarctic spring.

surface of interest. The chambers are separated by a sliding glass seal that can be opened to expose the cold surface to the reactants. The gas-phase contents of the cell were sampled with a mass spectrometer. Reactions on the cold surfaces were monitored by the changes in the mass scans that occurred when the sliding glass seal was opened. Reaction products that remained on the cold surface were detected subsequently by TDS, in which the partial pressures of the products were monitored as the temperature of the surface was increased slowly (3 K per minute). The ice and HCl-ice surfaces were prepared by condensation from the gas-phase onto a halocarbon wax-coated copper block held at 185 K. The  $\text{N}_2\text{O}_5$  was synthesized as described (14). A minor  $\text{HNO}_3$  impurity (<1%) was present in the  $\text{N}_2\text{O}_5$ . The  $\text{ClNO}_2$  used for mass identification and calibration was synthesized as described (10).

14. A mass scan at 1.0 mtorr of  $\text{N}_2\text{O}_5$  revealed no peaks

above *m/e* 62 [see L. Brouwer, M. J. Rossi, D. M. Golden, *J. Phys. Chem.* **90**, 4599 (1986)]. A small peak at *m/e* 48, possibly due to ozone impurity, was observed.

15. The sticking coefficient is given by

$$\gamma = (A_h/A_s) [(I^0 - I)/I]$$

where  $A_h$  and  $A_s$  are the areas of the Knudsen cell escape aperture and the surface area of the copper block, respectively, and  $I^0$  and  $I$  are the  $\text{N}_2\text{O}_5$  mass spectrometer signals in the absence and presence of the surface, respectively (13).

16. R. R. Friedl, J. H. Goble, S. P. Sander, *Geophys. Res. Lett.* **13**, 1351 (1986).

17. Supported under NSF grant ATM-8600764 and NASA contract NASW-3888.

18 December 1987; accepted 10 March 1988

## Evidence for Highly Reflecting Materials on the Surface and Subsurface of Venus

R. F. JURGENS, M. A. SLADE, R. S. SAUNDERS

Radar images at a 12.5-centimeter wavelength made with the Goldstone radar interferometer in 1980 and 1986, together with lunar radar images and recent Venera 15 and 16 data, indicate that material on the surface and subsurface of Venus has a Fresnel reflectivity in excess of 50 percent. Such high reflectivities have been reported on the surface in mountainous regions. Material of high reflectivity may also underlie lower reflectivity surficial materials of the plains regions, where it has been excavated by impact cratering in some areas.

**R**ADAR AND RADIOMETRIC DATA from the Pioneer Venus spacecraft indicate that several regions on Venus have both high Fresnel reflectivity and low radiometric emissivity ( $I$ ). These anomalies are typically associated with mountainous terrain, which has slightly cooler temperatures and increased surface roughness relative to the plains. The lowest emission temperatures reported (about 405 K) were much too low to have been caused by the difference in elevation between the mountains and the plains. Effective dielectric constants that could reduce the emissivity must be large, on the order of 30. Such high values are larger than those expected for basalt and most other nonigneous rocks. Pyrite inclusions in the rocks have been suggested as a mechanism to increase the conductivity of the material sufficiently to increase the reflectivity and reduce the emissivity ( $I$ ).

We provide radar evidence that material with high Fresnel reflectivity also occurs in the low plains regions where the temperature is near 735 K. We examined radar images that were made with the Goldstone triple interferometer during the inferior conjunctions of 1980 and 1986. The observa-

tions were made at a wavelength of 12.5 cm with circularly polarized waves. Right-circular polarization was transmitted, and left-circular polarization was received; this method captures the waves scattered by the quasi-specular scattering mechanism. We concentrated on images from regions within  $5^\circ$  to  $7^\circ$  of the subradar point because these images have the highest possible signal-to-noise ratio. The data acquisition and data processing procedures are given in (2), except that high-resolution, digital-acquisition equipment was used during the 1986 observations. This equipment substantially improved the best linear resolution of our images from about 8 km to about 1.3 km without serious loss of coverage.

Several of our reduced radar images show bright features that extend through a range of incidence angles of several degrees. The contrast of these features relative to their environs remains nearly constant with angle. These bright features are most easily explained by large values of the Fresnel reflection coefficient on the surface. The most striking is a large bright feature in the northern hemisphere that extends over an angular range from roughly  $3^\circ$  to  $7^\circ$  (Fig. 1A). The radar albedo locally is nearly four times as great as the average surface albedo (3). Although the companion altimetry image (Fig. 1B) for the region suffers from

### REFERENCES AND NOTES

- S. Solomon, R. R. Garcia, F. S. Rowland, D. J. Wuebbles, *Nature* **321**, 755 (1986).
- O. B. Toon, P. Hamill, R. P. Turco, J. Pinto, *Geophys. Res. Lett.* **13**, 1284 (1986); P. Hamill, O. B. Toon, R. P. Turco, *ibid.*, p. 1288; M. P. McCormick and C. R. Trepte, *ibid.*, p. 1276.
- P. J. Crutzen and F. Arnold, *Nature* **324**, 651 (1986); P. J. Crutzen, C. Bruhl, U. Schmailzl, F. Arnold, in *Aerosols and Climate*, M. P. McCormick and P. V. Hobbs, Eds. (A. Deepak, Hampton, VA, in press).
- M. B. McElroy, R. J. Salawitch, S. C. Wofsy, *Geophys. Res. Lett.* **13**, 1296 (1986).
- S. C. Wofsy, M. J. Molina, R. J. Salawitch, L. E. Fox, M. B. McElroy, *J. Geophys. Res.* **93**, 2442 (1988).
- J. C. Farman, B. G. Gardiner, J. D. Shanklin, *Nature* **315**, 207 (1985); M. B. McElroy, R. J. Salawitch, S. C. Wofsy, J. A. Logan, *ibid.* **321**, 759 (1986); L. T. Molina and M. J. Molina, *J. Phys. Chem.* **91**, 433 (1987); J. M. Rodriguez, M. K. W. Ko, N. D. Sze, *Geophys. Res. Lett.* **13**, 1292 (1986). For a general review, see R. J. Cicerone, *Science* **237**, 35 (1987).
- M. J. Molina, T.-L. Tso, L. T. Molina, F. C.-Y. Wang, *Science* **238**, 1253 (1987).
- M. A. Tolbert, M. J. Rossi, R. Malhotra, D. M. Golden, *ibid.*, p. 1258.
- M. T. Leu, *Geophys. Res. Lett.* **15**, 17 (1988).
- H. H. Nelson and H. S. Johnston, *J. Phys. Chem.* **85**, 3891 (1981).
- These reactions have been reported to occur on laboratory surfaces. See, for example: E. C. Tuazon, R. Atkinson, C. N. Plum, A. M. Winer, J. N. Pitts, Jr., *Geophys. Res. Lett.* **10**, 953 (1983); C. A. Cantrell, J. A. Davidson, R. E. Shetter, B. A. Anderson, J. G. Calvert, *J. Phys. Chem.* **91**, 6017 (1987).
- W. F. J. Evans, C. T. McElroy, I. E. Galbally, *Geophys. Res. Lett.* **12**, 825 (1985).
- For a general review of the experimental technique, see D. M. Golden, G. N. Spokes, S. W. Benson, *Angew. Chem. Int. Ed. Engl.* **12**, 534 (1973). The Knudsen cell used in the present experiment consists of two chambers, one of which contains the cold

Jet Propulsion Laboratory, California Institute of Technology, 4800 Oak Grove Drive, Pasadena, CA 91109.

minor systematic traces of the interferometer fringe pattern, the feature does possess some slight topography. The eastern part of the feature contains a ridge, whereas an isolated mound occurs to the west. The topography in both areas rises to around 1 km above the surroundings, with leading edge regional slopes between  $0.25^\circ$  and  $0.5^\circ$ . The area between the ridge and the mound is flat even though it also has high reflectivity. Therefore, the high albedo is probably not associated with slope-induced scattering from the front edge of the inclines. An alternative explanation for the scattering behavior requires that facets in the 10- to 100-m size are preferentially directed toward the observer for each angle of incidence. Such a fortuitous situation is unlikely. However, some combination of high Fresnel reflectivity and slope-induced scattering remains possible.

Even with the presence of this large bright feature, the regional scattering properties of this plains area are characterized by a relatively small root-mean-square (rms) slope. We compared the scattering law for this image with the scattering law predicted from the model by Hagfors (4) with various values of the surface roughness parameter,  $C$  (Fig. 2). A value for  $C$  of 250 gives a good fit to the observed law for our data and indicates that the rms slope is about  $4^\circ$  (which equals  $C^{-0.5}$  radian).

During the 1986 inferior conjunction of Venus, additional observations were made that had a best resolution of 1.3 km. The image shown in Fig. 3 covers an angular range to about  $4.5^\circ$  and is therefore entirely in the part of the scattering law in which larger  $C$  values (smaller rms slopes) increase the albedo (Fig. 2). Thus, rough

areas appear darker than the average surface. The western and southern parts of the image contain extensive bright regions that show considerable kilometer-scale structure. The image becomes featureless to the north and east. Measurements of the bright structure indicate that its albedo is enhanced as much as four to five times the average surface albedo. In the upper part of Fig. 3, there are two dark circular regions that have either a bright extension or a well-defined halo. The western feature appears to have bright material overlying the southern part of the dark spot. The eastern feature has the morphology of an impact crater. The origin of the more western feature is less certain, but its similarity to the other could indicate a similar origin. Two similar impact structures in close proximity were unexpected; therefore, we cannot rule out the possibility that these features are volcanic calderas. In either case, rough rings would be expected. The halo is bright, not dark as would be expected for a rough crater rim at this angle of incidence and observed in the opposite sense of polarization. The bright halo indicates that the material must have a high Fresnel reflectivity to overcome the darkening that would occur because of the roughness around the rim of the crater. We suggest that the feature is either an impact or volcanic crater and that the rim contains radar-bright material from below the surface. If the crater is impact in origin, we would argue that because radar-bright material appears plentiful to the west, less reflecting material likely covers the region to the east. Additionally, the entire southwestern part of the figure may expose radar-bright material that has been swept clean of regolith. If the crater is volcanic, we would suggest that much of the bright

material is volcanic in origin and mantles the darker surface material.

Radar images made by the Venera 15 and 16 synthetic aperture radar show craters that are similar in size to the craters discussed above but at much more northerly latitudes. Ivanov *et al.* indicate that 25% of the Venera craters have bright halos (5). The halos extend roughly  $1.8 \pm 0.5$  times the crater diameter outward from the crater's center. A few craters have dark outer halos as well. The angle of incidence of the Venera images is near  $10^\circ$ , and thus these images likely show slope enhancements that are similar to those of the Goldstone images. Many of the Venera craters have slope enhancements but lack bright halos. Ivanov *et al.* attributed the bright halos of the craters that have them to increased surface roughness; the dark outer ring they attributed to a shock smoothing process. If we assume that Hagfors scattering model is a good representation of the surface and the average  $C$  parameter is near 250, then rougher surfaces that have  $C$  parameters as low as 25 would not show substantial brightening. Bright halos might be seen against a significantly smoother surface if such surfaces occur on Venus. (They might also be visible in regions having atypical scattering properties.) Most likely, the bright halos are the result of ejecta material that has higher Fresnel reflectivity. The dark outer halos may be the result of shock smoothing as proposed (5) or the product of weathering of ejecta material that has been blown from the surface. Such material might be more porous than the normal surface material and yield a lower Fresnel reflectivity. Alternately, the distal ejecta may be extremely fine and tend to fill in and smooth the surface. Radar-bright

**Fig. 1. (A)** Radar reflectivity image of a small region of Venus that shows a structure with very high reflectivity (12). The best resolution is approximately 8 km. The reflectivity image shows that the ratio of the observed power to the expected power follows the measured scattering law (dots, Fig. 2). The longitude reference for Goldstone images is given in (2). To obtain International Astronomical Union longitude, add  $\sim 4^\circ$  to the longitude shown. **(B)** Radar altimetry image of the region of (A). The range in elevation from dark to light areas is  $-2$  to 1 km relative to the radius at the subradar point. Some artifacts of the processing are visible as horizontal bands, and noise degrades the image radially outward from the center. The altitude errors vary from 40 m near the center to around 400 m at the edges.

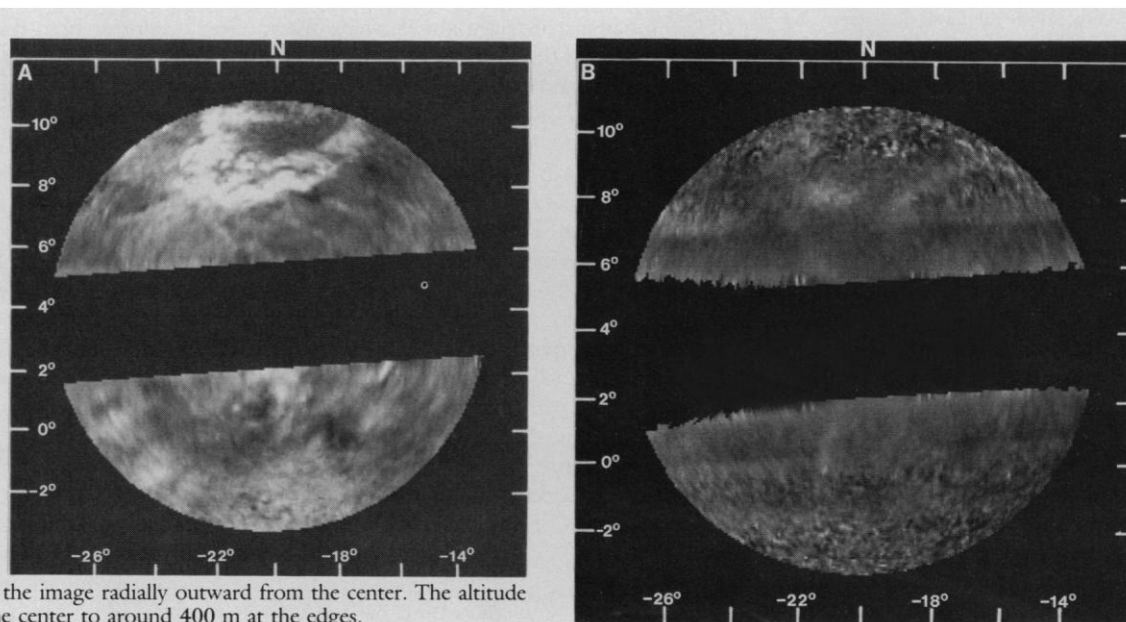


**Fig. 2.** The radar cross section,  $\sigma(\theta)$ , per unit surface area at angles of incidence and observation,  $\theta$ , as predicted by Hagfors' model (4). The solid lines are for the case of a Fresnel reflection coefficient,  $\rho_0$ , of unity and demonstrate how changes in surface roughness ( $C$  parameter) affect the scattering law. The dashed curve shows the best fit to the data (dots) from 2 July 1980; the coefficient  $\rho_0$  is 0.125 and  $C$  is 250.

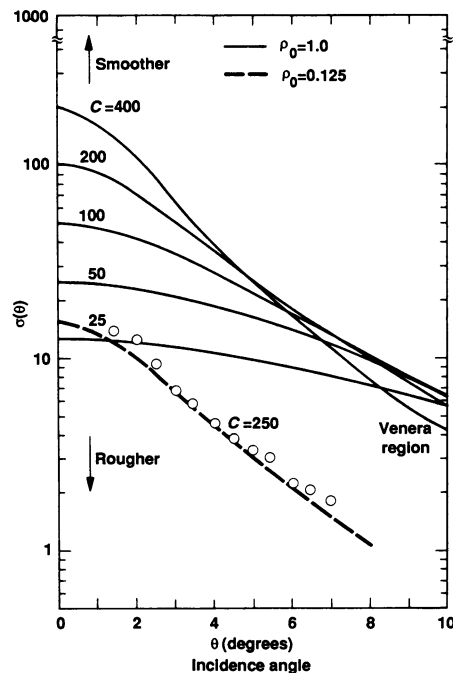
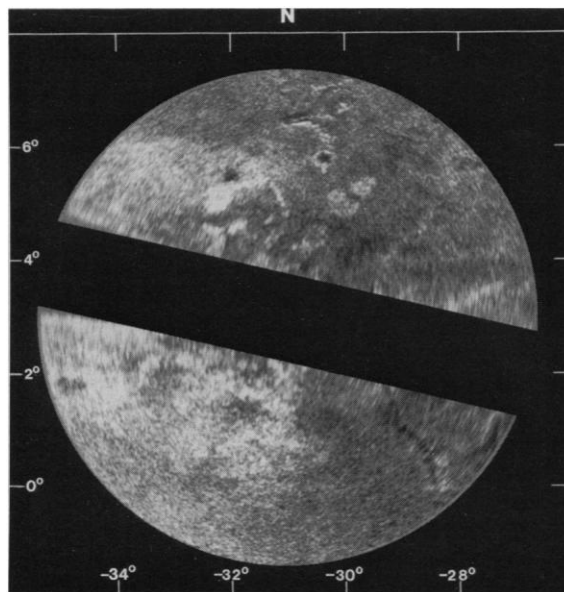


**Fig. 3.** Radar reflectivity image at 1.3-km best resolution of a region farther east from the one in Fig. 1 that has regions with high reflectivity and a bright crater ring. The largest incidence angle is about  $4.5^\circ$ . The data are normalized in the same manner as in Fig. 1A. The altimetry image is not shown.



rings have been observed at large angles of incidence where the quasi-specular scattering component nearly vanishes, which leaves the predominant diffuse scattering from the rings (6).

Additional evidence of radar-bright ejecta from the 70-cm lunar radar maps of Thompson and co-workers (7) and the 3.8-cm maps of Zisk *et al.* (8) indicates that bright rings or halos are common in the depolarized maps for incidence angles less than  $15^\circ$  (9). The polarized component in this angular range has slope-induced enhancements from the crater walls and facing rims, but complete rings are observed only around the crater Copernicus. Copernicus is perhaps a special case where dense rock is contrasted against the radar-dark mare at an angle of

incidence for which roughness could brighten the ring. We conclude that lunar craters rarely show bright ejecta at small angles of incidence when observed in the polarized mode.

Radar-bright rings or halos associated with Venusian craters that have been observed at small angles of incidence are unlikely to be a result of increased surface roughness. Neither theoretical scattering laws nor radar images of lunar craters indicate that surface roughness can be a significant mechanism for generating bright rings at angles of incidence less than  $10^\circ$ . For example, two Venusian craters in the 1978 Goldstone series of observations show dark rings at small incidence angles (10), which indicates that not all craters have bright

rings. The radar-bright rings are most likely the result of ejecta or volcanic material from the subsurface having high Fresnel reflectivity. Such material is apparently widespread in some regions of Venus where it occurs on the surface. The material is also apparently common in the highlands as well, where it causes distinct emission anomalies. The Venera 15 and 16 data indicate that many craters with bright halos are widely distributed on plains regions in the northern hemisphere. Thus, we conclude that the material is widespread, chemically stable (11) on the surface, and probably covered by a lower reflective blanket (possibly basaltic) in many other regions and perhaps globally.

#### REFERENCES AND NOTES

1. G. H. Pettengill, P. G. Ford, S. Nozette, *Science* 217, 640 (1982); P. G. Ford and G. H. Pettengill, *ibid.* 220, 1379 (1983).
2. R. F. Jurgens *et al.*, *J. Geophys. Res.* 85, 8282 (1980).
3. The Fresnel reflectivity for the "average" surface from both the Pioneer Venus Orbiter maps and these observations is on the order of 0.12 in this region.
4. T. Hagfors, *J. Geophys. Res.* 69, 3779 (1964).
5. B. A. Ivanov *et al.*, *ibid.* 91, D413 (1986).
6. D. B. Campbell and B. A. Burns, *ibid.* 85, 8271 (1980).
7. T. W. Thompson *et al.*, *Icarus* 46, 201 (1981); T. W. Thompson, R. S. Saunders, D. E. Weissman, *Earth Moon Planets* 36, 167 (1986); T. W. Thompson, *ibid.* 37, 59 (1987).
8. See p. 34 of S. H. Zisk *et al.*, *The Moon* 10, 17 (1974).
9. These image sets have been made in two circular polarizations so that small-scale roughness in the ring or halo can be detected even at small angles of incidence. Unfortunately, there is little surface coverage at low angles of incidence, and the coverage that is available is near the center of the lunar disk where the range resolution is poor.
10. R. F. Jurgens, unpublished data; available to interested persons via magnetic tape or diskette.
11. If 25% of Venusian craters have bright ejecta and the mean surface age is 1 billion years, then we can speculate that weathering to reduce brightness takes about 250 million years (5).
12. The relative accuracy of an image pixel depends on the number of spectra averaged (if a high signal-to-noise ratio is assumed). For this image the number of spectra is 180, which gives a relative error of 7%. The relative accuracy of the 1986 images is less than that for the 1980 to 1982 images because the higher spatial resolution of the 1986 images decreases the signal-to-noise ratio and longer coherent integration times produced higher spectral resolution. The image in Fig. 3 is based on 21 spectra, and each pixel has a relative error of about 22%. The absolute calibration error for the 1980 to 1982 images, if the full error budget is considered, is about 10%. In 1986, the system performance was degraded by about 3 dB compared to its 1980 level. Details on accuracies are in R. F. Jurgens, internal office memo IOM 79-016A (Jet Propulsion Laboratory, 1979).
13. This research was carried out by the Jet Propulsion Laboratory, California Institute of Technology, under contract with NASA. We thank R. R. Green and C. Franck, who cared for the data acquisition system during the 1980 observations and G. A. Morris, S. Brokl, L. Robinett, C. Franck, and K. H. Farazian, who helped develop the new data acquisition system used for the 1986 observations. We also thank the Development Radio Astronomy Unit at Goldstone, who carried out the observing program, and E. M. Standish, who provided the tracking ephemeris products for all observations. We thank P. Ford for discussions on the Pioneer Venus Orbiter data.

21 January 1988; accepted 11 April 1988